a small negative fourth-order contribution in the expansion of λ_c.

6. CONCLUSION

The present neutron-diffraction study has yielded the following additional information about the magnetic structures of Tb.

(a) The magnetic long-range order follows the characteristic temperature variation of spontaneous magnetization with $T_N = 226°\text{K}$. For temperatures above $0.9T_N$ there is good agreement with the power law $(T_N - T)^\beta$ with $\beta = \frac{1}{3}$ except in a region few degrees below T_N where $\beta = \frac{1}{4}$. The transition between the ferromagnetic and spiral phase is of first order and occurs at 216°K without any change of the long-range order.

(b) The spiral turn angle per layer has a minimum at the ferromagnetic to spiral transition temperature. This is in agreement with the superzone theory which predicts that the turn angle should decrease with increase of spiral long-range order. The quantitative agreement between theories based on the free-electron model and the experiment is poor, but this is not surprising since the rare earths are known to have electronic structures very different from the free-electron model.

(c) The ferromagnetic long-range order $\langle s \rangle$ has been correlated with the lattice expansion λ_c due to magnetostriction, and reasonable agreement with the approximate relation $\lambda_c = kg^2\mu^2 \langle s \rangle^2$ was observed.

ACKNOWLEDGMENT

The authors wish to express their gratitude to Professor A. R. Mackintosh for valuable discussions and criticism.

PHYSICAL REVIEW VOLUME 162, NUMBER 2 10 OCTOBER 1967

Nuclear Spin-Lattice Relaxation in Hexagonal Transition Metals: Titanium†

ALBERT NARATH
Sandia Laboratory, Albuquerque, New Mexico

(Received 15 May 1967)

The nuclear magnetic resonance of ^{47}Ti and ^{49}Ti has been observed in hexagonal close-packed titanium metal in the temperature range $T = 1$–$4°\text{K}$. Measurements of the line profile and relaxation rates were carried out at 12.5 MHz by pulsed nuclear resonance techniques. Since the gyromagnetic ratios of ^{47}Ti and ^{49}Ti are nearly identical, the resonances of the two isotopes were superimposed. A partially resolved first-order quadrupole spectrum having a total width exceeding 8 kOe was observed, yielding a probable assignment $h^{-1}e^2qQ^{47} \approx h^{-1}e^2qQ^{49} \approx 7.7$ MHz. The average Knight shift is estimated to be $K = (+0.4 \pm 0.2)\%$. The spin-lattice relaxation times T_1, which are quite long ($T_1T = 150 \pm 20$ sec°K), provide evidence that the conduction-electron states at the Fermi level are predominantly d-like. The theory of nuclear spin-lattice relaxation in hexagonal transition metals is treated in the tight-binding approximation. Contact, core-polarization, orbital, and dipolar hyperfine interactions are considered. The magnitudes of the orbital and dipolar contributions to the spin-lattice relaxation rate depend on the orientation of the magnetic field relative to the hexagonal c axis. In the presence of s-d mixing, the contact contribution is found to interfere destructively with one of the components of the core-polarization contribution. The predicted total relaxation rates are shown to depend more strongly on the orbital admixture coefficients than is the case in cubic transition metals. The relatively large number of parameters in the theory precludes a unique fit to the experimental results for titanium. In general, however, the calculated rates exceed the observed rate by a factor of 2–3 over a wide range of parameter values. The apparent discrepancy is attributed to the combined effects of (1) the electron-phonon enhancement of the electronic specific heat and (2) s-d interference effects. The former effect causes the "bare" electron density of states to be overestimated, while the latter leads to an overestimate of the sum of contact and core-polarization contributions to the relaxation.

I. INTRODUCTION

DURING recent years considerable progress has been achieved in the utilization of conduction-electron-induced nuclear spin-lattice relaxation phenomena in the study of electronic properties of transition metals. To date, most theoretical and experimental efforts in this field have been concerned with metals having cubic structures. The important contributions to the observed relaxation rates have been shown to arise from core-polarization[1] and orbital[2] hyperfine interactions with the d component of the conduction-electron wave functions at the Fermi level, as well as from the familiar contact[3] hyperfine interaction with the s component. Conduction-electron contributions associated with magnetic-dipole[2] and electric-quadrupole[4,5] hyperfine interactions, on the other hand, are

---

† This work was supported by the U.S. Atomic Energy Commission.

[1] Y. Yafet and V. Jaccarino, Phys. Rev. **133**, A1630 (1964).

[2] Y. Obata, J. Phys. Soc. Japan **18**, 1020 (1963).

[3] J. Korringa, Physica **16**, 601 (1950).

[4] A. H. Mitchell, J. Chem. Phys. **26**, 1714 (1957).

[5] Y. Obata, J. Phys. Soc. Japan **19**, 2348 (1964).

usually quite small. In the tight-binding approximation, the total relaxation rate can be expressed in analytical form.[1,2] Moreover, since spin-orbit effects are generally assumed to be small, no interference terms arise in the cubic case among the various interactions. The relaxation rate in cubic transition metals is therefore given by a sum of the individual hyperfine contributions. The detailed application of the theory to experimental data unfortunately requires a knowledge of several classes of parameters relating to conduction-electron properties appropriately averaged over the Fermi surface. These are (1) the relevant hyperfine interaction parameters, (2) the total bare-electron density of states, (3) the weights of the *s* and *d* components of the conduction-electron wave function, and (4) the point-group symmetry properties of the *d* component (i.e., the ratio of the Γ_3 and Γ_5 orbital admixtures). The dependence of the calculated rate on the fourth parameter is weak since the variation of the core-polarization contribution with the Γ_3/Γ_5 admixture coefficient is nearly cancelled in most cases by that of the orbital contribution. Information concerning the remaining parameters can often be obtained by combining nuclear relaxation data with the results of related measurements. For example, it is often possible to derive reasonably accurate values of the hyperfine constants from the respective free-atom values. If the density of states can be estimated from the measured electronic specific heat, an approximate value for the average *s*/*d* ratio at the Fermi level can then be inferred from the experimental relaxation rates.[6,7] Conversely, if the *s*/*d* ratio is known, it is possible, in principle, to obtain an estimate of the electron-phonon enhancement of the electronic specific heat. The complex dependence of the nuclear spin-lattice relaxation rate on the details of the electronic structure is of course similar to the complexities associated with most transition-metal properties.

The present study is concerned with nuclear spin-lattice relaxation in hexagonal close-packed (hcp) transition metals. The primary purpose of this work is to examine the additional theoretical and experimental complications which are introduced by the lower crystal symmetry. Of particular interest are questions relating to the possible importance of anisotropy and interference effects in the relaxation rate. The dependence of the relaxation rate on the symmetry properties of the conduction-electron wave functions at the Fermi level is examined in detail. The extent to which the theory can be applied at present to experimental data is illustrated by means of a comparison between observed and calculated rates for titanium metal. In addition, data concerning the quadrupole splittings and Knight shifts of ^{47}Ti and ^{49}Ti in titanium metal are presented.

In Sec. II the theory of spin-lattice relaxation in hexagonal crystals is treated in the tight-binding approximation. The experimental techniques used in the present study are described in Sec. III. The results of our experimental measurements on titanium metal are presented and analyzed in Sec. IV and discussed in Sec. V. The rate equations which describe the magnetic hyperfine induced spin-lattice relaxation processes for nuclear spins $I=\frac{5}{2}$ and $I=\frac{7}{2}$ are given in the Appendix.

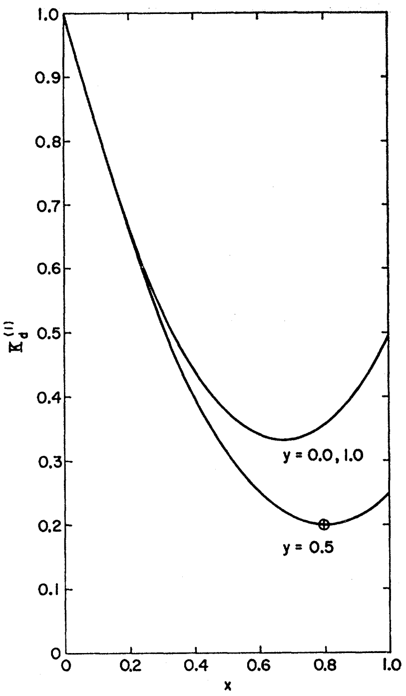

FIG. 1. Plot of the *d*-spin core-polarization reduction factor $K_d^{(1)}$ for hexagonal symmetry as a function of the orbital admixture parameters *x* and *y*. The two curves indicate the range of possible values of $K_d^{(1)}$. The circled cross identifies the value of $K_d^{(1)}$ appropriate for a spherical Fermi surface.

II. THEORY OF SPIN-LATTICE RELAXATION

Following Obata,[2] we calculate the relaxation rate by treating the magnetic hyperfine interactions in terms of an effective-spin Hamiltonian

$$\mathcal{H}=-\gamma_n\hbar\mathbf{I}\cdot\mathbf{h},\tag{2.1}$$

where γ_n is the nuclear gyromagnetic ratio and $\mathbf{I}$ is the nuclear-spin angular-momentum operator. The effective-field operator $\mathbf{h}$ is composed of *s*-contact ($\mathbf{h}_s$), *d*-spin core-polarization ($\mathbf{h}_d$), *d*-spin dipolar ($\mathbf{h}_{\text{dip}}$), and *d*-orbital ($\mathbf{h}_{\text{orb}}$) terms.

$$\mathbf{h}=\mathbf{h}_s+\mathbf{h}_d+\mathbf{h}_{\text{dip}}+\mathbf{h}_{\text{orb}},\tag{2.2}$$

with

$$\mathbf{h}_s=-2H_{\text{hfs}}^{(s)}\mathbf{s}_s,\tag{2.3}$$

$$\mathbf{h}_d=-2H_{\text{hfs}}^{(s)}\mathbf{s}_d,\tag{2.4}$$

$$\mathbf{h}_{\text{dip}}=-\gamma_e\hbar r^{-3}[\mathbf{s}_d-3r^{-2}(\mathbf{r}\cdot\mathbf{s}_d)\mathbf{r}],\tag{2.5}$$

$$\mathbf{h}_{\text{orb}}=-\gamma_e\hbar r^{-3}\mathbf{l},\tag{2.6}$$

---

[6] A. Narath and A. T. Fromhold, Jr., Phys. Rev. **139**, A794 (1965).

[7] A. Narath and D. W. Alderman, Phys. Rev. **143**, 328 (1966).

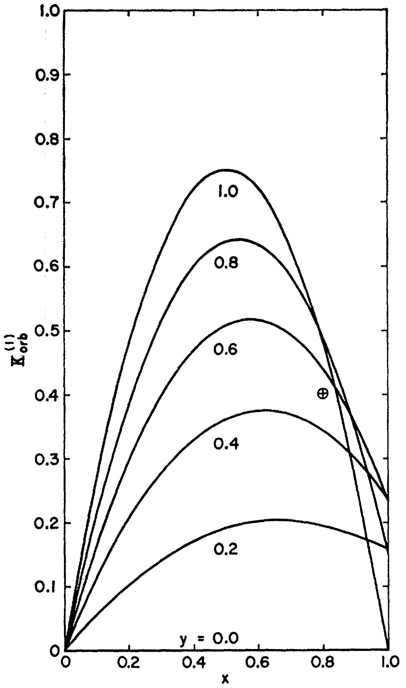

FIG. 2. Plot of the d-orbital reduction factor $K_{orb}^{(1)}$ for hexagonal symmetry ($\mathbf{H} \| c$) as a function of the orbital admixture parameters x and y. The circled cross identifies the spherical case as in Fig. 1.

where γ_e is the electronic gyromagnetic ratio, $\mathbf{s}_s$ and $\mathbf{s}_d$ are the s-spin and d-spin angular-momentum operators ($s=\frac{1}{2}$) for the conduction electrons, respectively, $\mathbf{l}$ is the orbital-angular-momentum operator for the d electrons ($l=2$), and r is the appropriate electronic position coordinate. We have assumed that the electronic g value may be taken as 2. Although the effect of the dipolar interaction on the relaxation rate is generally small, we include it in our discussion for the sake of completeness. The effective s-contact and core-polarization (d-spin) hyperfine fields per electron are denoted by $H_{\text{hfs}}^{(s)}$ and $H_{\text{hfs}}^{(d)}$, respectively. The expectation value of r^{-3} in (2.5) and (2.6) can be expressed in terms of an orbital hyperfine field per unit orbital angular momentum $H_{\text{hfs}}^{(\text{orb})} = -\gamma_e \hbar \langle r^{-3} \rangle$. Straightforward application of first-order time-dependent perturbation theory to (2.1) yields a relaxation rate for a given site in the crystal

$$T_1^{-1} = (\pi/\hbar)(\gamma_n \hbar)^2 \sum_{\mu\mu'} \sum_{\mathrm{kk}'} \sum_{\sigma\sigma'} | \langle \mu'\mathbf{k}'\sigma' \mid h^- \mid \mu\mathbf{k}\sigma \rangle |^2$$
$$\times f_{\mu\mathbf{k}\sigma}(1 - f_{\mu'\mathbf{k}'\sigma'})\delta(\Delta E), \quad (2.7)$$

where μ, $\mathbf{k}$, and σ are the band, wave vector, and spin indices, respectively, $f_{\mu\mathbf{k}\sigma}$ is the occupation number of the one-electron Bloch state $| \mu\mathbf{k}\sigma \rangle$, and the δ function $\delta(\Delta E)$ expresses the energy conservation requirements for the relaxation process. In the tight-binding approximation, the conduction-electron wave functions are constructed from atomic orbitals. For a lattice with an arbitrary basis the result is

$$\Psi_{\mu\mathbf{k}\sigma}(\mathbf{r}) = N^{-1/2} \sum_j \sum_p \exp(i\mathbf{k}\cdot\mathbf{R}_j)$$
$$\times \exp(i\mathbf{k}\cdot\mathbf{R}_p) a_{\mu\mathbf{k}}(\mathbf{r} - \mathbf{R}_{jp})\phi_\sigma, \quad (2.8)$$

where N denotes the number of unit cells in the crystal, $\mathbf{R}_j$ specifies the location of a given unit cell, $\mathbf{R}_p$ specifies the atomic positions within the unit cell, and $\mathbf{R}_{jp} = \mathbf{R}_j + \mathbf{R}_p$. The ϕ_σ are spin functions, while the $a_{\mu\mathbf{k}}(\mathbf{r} - \mathbf{R}_{jp})$ are linear combinations of atomic orbitals (LCAO) defined by

$$a_{\mu\mathbf{k}}(\mathbf{r} - \mathbf{R}_{jp}) = \sum_m c_{\mu m\mathbf{k}p} \phi_m(\mathbf{r} - \mathbf{R}_{jp}), \quad (2.9)$$

where the $c_{\mu m\mathbf{k}p}$ are elements of a unitary transformation and the $\phi_m(\mathbf{r} - \mathbf{R}_{jp})$ are atomic functions which form bases for irreducible representations of the point group appropriate for the position $\mathbf{R}_{jp}$. We also note that the functions (2.8) are not normalized unless all overlap integrals between LCAO functions centered on different sites vanish.

In keeping with the symmetry properties of the hcp structure, we assume in the following that the symmetry elements of all nonequivalent atomic positions correspond to the same subgroup of the crystallographic point group. It can then be readily shown that the symmetry properties of the transformation coefficients are expressed by

$$c_{\mu m(G\mathbf{k})p} = \sum_{m'=\Gamma(m)} c_{\mu m'\mathbf{k}p} D^{\Gamma}{}_{m'm}(G), \quad (2.10)$$

where G is an operation of the local point group and $m' = \Gamma(m)$ means all m' belonging to the same irreducible representation as does m. The $D^{\Gamma}{}_{mm'}(G)$ are elements of the appropriate transformation matrix which satisfy the standard orthogonality relation

$$\sum_G D^{\Gamma}{}_{mm'}(G) D^{\Gamma}{}_{m''m'''}(G)^* = \delta_{mm''}\delta_{m'm'''}(g/g^{\Gamma}), \quad (2.11)$$

where g is the order of the group and g^{Γ} is the dimensionality of the representation Γ.

The matrix elements in (2.7) can now be evaluated by expanding the Bloch functions according to the tight-binding prescription (2.8). We assume that matrix elements between orbitals centered on different atoms can be neglected. This assumption is generally justified and is, moreover, consistent with the neglect of normalization in the tight-binding functions. Using (2.9)–(2.11), together with the fact that $E_{\mu G\mathbf{k}} = E_{\mu\mathbf{k}}$, we find the following relaxation rate for the pth site.

$$T_1(p)^{-1} = (\pi/\hbar N^2)(\gamma_n \hbar)^2 k_B T$$
$$\times \sum_{\mu\mu'} \sum_{\mathrm{kk}'} \sum_{\sigma\sigma'} \delta(E_{\mu\mathbf{k}} - E_{\mu'\mathbf{k}'}) \delta(E_{\mu\mathbf{k}} - E_F)$$
$$\times \sum_{mm'} F_{\mu\mathbf{k}p}{}^{\Gamma(m)} F_{\mu'\mathbf{k}'p}{}^{\Gamma(m')} \mid \langle m'\sigma'p \mid h^- \mid m\sigma p \rangle|^2, \quad (2.12)$$

where k_B is Boltzmann's constant, E_F is the Fermi energy, and the $F\mu_{\mathrm{k}p}{}^{\Gamma(m)} \equiv | c_{\mu m\mathrm{k}p} |^2$ are fractional admixture coefficients which have the same value for all m forming a basis for a given irreducible representation $\Gamma(m)$. By defining average values of the $F_{\mu\mathrm{k}p}{}^{\Gamma(m)}$ according to

$$F_p{}^{\Gamma(m)} = \sum_{\mu} \sum_{\mathrm{k}} F_{\mu\mathrm{k}p}{}^{\Gamma(m)} [\delta(E_{\mu\mathrm{k}} - E_F)][N(0)N]^{-1}, \quad (2.13)$$

where the product $N(0)N$ is the total number of states per unit energy interval at the Fermi level for one direction of the spin, we can write (2.12) in the form

$$T_1(p)^{-1} = (\pi/\hbar)(\gamma_n\hbar)^2 k_B T [N(0)]^2$$
$$\times \sum_{mm'} \sum_{\sigma\sigma'} F_p{}^{\Gamma(m)} F_p{}^{\Gamma(m')} | \langle m'\sigma' p | h^- | m\sigma p \rangle |^2. \quad (2.14)$$

By definition, the factors $F_p{}^{\Gamma(m)}$ are normalized to unity

$$\sum_{m} \sum_{p} F_p{}^{\Gamma(m)} = 1. \quad (2.15)$$

We wish to apply (2.14) to the hcp structure. The relevant point group is D_{6h} which is conveniently expressed as the direct product group $D_{6h} = D_{3h} \times I$. The hcp lattice contains two atoms per unit cell in special positions which are related by operations of the space group ($P6_3$/mmc). With the origin placed at either of the two sites, the covering operations of the lattice correspond to D_{3h}, which is clearly a subgroup of D_{6h}. The nuclear resonance properties of the two nonequivalent atoms are identical. The distinction between these sites can therefore be ignored if N in (2.13) is defined as the number of atoms in the crystal. In other words, we may limit our discussion to a primitive lattice with D_{3h} point-group symmetry and therefore drop the p subscript. The nonvanishing matrix elements of (2.14) which arise from the hyperfine-interaction terms (2.3)–(2.6) involve the s-like ($l=0$) atomic function which transforms as the A_1' representation of D_{3h}, and the five d-like ($l=2$) functions which form bases for the irreducible representations A_1', E', and E''. The appropriate decomposition of the $l=2$ representation of the three-dimensional rotation group leads to symmetry functions whose angular parts are given in real form by

$$A_1' : Y_2{}^0(\alpha, \beta), \quad (2.16)$$

$$E' : -2^{-1/2} i [Y_2{}^2(\alpha, \beta) - Y_2{}^{-2}(\alpha, \beta)],$$
$$2^{-1/2} [Y_2{}^2(\alpha, \beta) + Y_2{}^{-2}(\alpha, \beta)], \quad (2.17)$$

$$E'' : -2^{-1/2} [Y_2{}^1(\alpha, \beta) - Y_2{}^{-1}(\alpha, \beta)],$$
$$2^{-1/2} i [Y_2{}^1(\alpha, \beta) + Y_2{}^{-1}(\alpha, \beta)], \quad (2.18)$$

where the $Y_2{}^q(\alpha, \beta)$ are normalized spherical harmonics of order two. The polar angle α is measured with respect to a Z axis which is chosen to lie parallel to the crystallographic c axis. The positions of the X and Y axes in the hexagonal basal plane are arbitrary.

The calculation of the relaxation rate (2.14) is now easily accomplished. We assume an external magnetic field oriented along a z direction whose polar and azimuthal angles in the X, Y, Z coordinate system are specified by θ and ϕ, respectively. The contact and core-polarization matrix elements can be obtained immediately since they are obviously independent of field orientation. The orientation dependence of the orbital and dipolar matrix elements is most conveniently obtained by expressing these interactions in spherical tensor form.

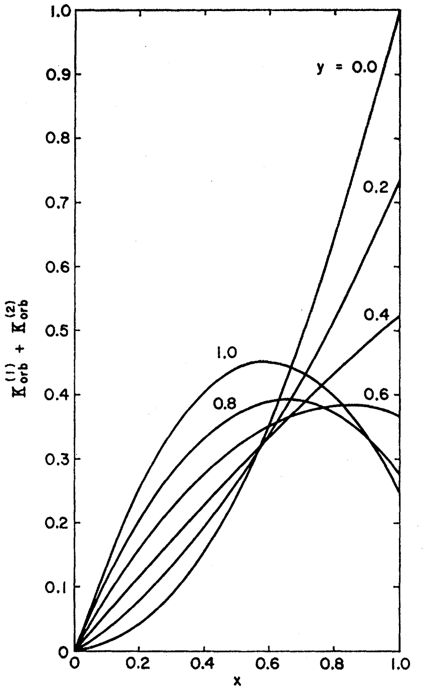

FIG. 3. Plot of the d-orbital reduction factor $\mathrm{K}_{\mathrm{orb}}{}^{(1)} + \mathrm{K}_{\mathrm{orb}}{}^{(2)}$ for hexagonal symmetry ($\mathbf{H} \perp c$) as a function of the orbital admixture parameters x and y.

$$h_{\mathrm{orb}}{}^- = 2^{1/2} \gamma_e \hbar r^{-3} L_1{}^{-1}(\alpha', \beta'), \quad (2.19)$$

$$h_{\mathrm{dip}}{}^- = 2(6\pi/5)^{1/2} \gamma_e \hbar r^{-3} [s^+ Y_2{}^{-2}(\alpha', \beta')$$
$$- 6^{-1/2} s^- Y_2{}^0(\alpha', \beta') + s^z Y_2{}^{-1}(\alpha', \beta')]. \quad (2.20)$$

Here α' and β' specify orientations in the x, y, z coordinate system. The connection between the Cartesian components of l and the tensor elements $L_1{}^q$ is given in the usual way by

$$L_1{}^{\pm 1} = \mp 2^{-1/2} l^{\pm} \equiv \mp 2^{-1/2} (l^x \pm i l^y), \quad (2.21)$$

$$L_1{}^0 = l^z. \quad (2.22)$$

The tensor elements which appear in (2.19) and (2.20) can now be transformed into the X, Y, Z system by making use of the well-known transformation properties of spherical tensors under rotations.

$$L_1{}^q(\alpha', \beta') = \sum_{q'} D^1{}_{qq'}(\theta, \phi, 0) L_1{}^{q'}(\alpha, \beta), \quad (2.23)$$

$$Y_2{}^q(\alpha', \beta') = \sum_{q'} D^2{}_{qq'}(\theta, \phi, 0) Y_2{}^{q'}(\alpha, \beta). \quad (2.24)$$

The $\mathbf{D}^l(\theta, \phi, 0)$ denote appropriate rotation matrices.[8] Performing the indicated transformations and evaluating the necessary matrix elements in the basis (2.16)–(2.18) reduces (2.14), in the absence of *s-d* mixing, to the form

$$R = (4\pi/\hbar)(\gamma_n\hbar)^2 k_B [(N(0)]^2 \sum_i P_i^2 (\mathrm{K}_i^{(1)} + \mathrm{K}_i^{(2)} \sin^2\theta), \quad (2.25)$$

where $R \equiv (T_1 T)^{-1}$ and the sum is taken over the four hyperfine interactions with

$$P_s = \rho H_{\mathrm{hfs}}^{(s)}, \quad (2.26)$$

$$P_d = (1-\rho) H_{\mathrm{hfs}}^{(d)}, \quad (2.27)$$

$$P_{\mathrm{dip}} = P_{\mathrm{orb}} = (1-\rho) H_{\mathrm{hfs}}^{(\mathrm{orb})}, \quad (2.28)$$

and ρ is the average fractional *s* character at the Fermi level.

$$\rho = N_s(0)/N(0). \quad (2.29)$$

[The effect on (2.25) due to any *p* admixture in the conduction-electron states at the Fermi level is discussed at the end of this section]. The reduction factors $\mathrm{K}_i^{(1)}$ and $\mathrm{K}_i^{(2)}$ are given by

$$\mathrm{K}_s^{(1)} = 1, \quad (2.30)$$

$$\mathrm{K}_s^{(2)} = 0, \quad (2.31)$$

$$\mathrm{K}_d^{(1)} = [1 - 2x + \tfrac{3}{2}x^2 - x^2 y(1-y)], \quad (2.32)$$

$$\mathrm{K}_d^{(2)} = 0, \quad (2.33)$$

$$\mathrm{K}_{\mathrm{orb}}^{(1)} = xy[3 - x(y+2)], \quad (2.34)$$

$$\mathrm{K}_{\mathrm{orb}}^{(2)} = \tfrac{1}{4}x[4x(1-y) - y(6-7xy)], \quad (2.35)$$

$$\mathrm{K}_{\mathrm{dip}}^{(1)} = (1/392)[8 + 32x - 36x^2 - 42xy + 52x^2y + 5x^2y^2], \quad (2.36)$$

$$\mathrm{K}_{\mathrm{dip}}^{(2)} = (3/784)[8 - 32x + 28x^2 + 18xy - 20x^2y - 7x^2y^2], \quad (2.37)$$

where

$$x = 2[F^{\Gamma(E')} + F^{\Gamma(E'')}][1-\rho]^{-1}, \quad (2.38)$$

$$y = F^{\Gamma(E'')}[F^{\Gamma(E')} + F^{\Gamma(E'')}]^{-1}, \quad (2.39)$$

and according to (2.15)

$$F^{\Gamma(A_1')} + 2F^{\Gamma(E')} + 2F^{\Gamma(E'')} = 1. \quad (2.40)$$

Thus, if *s-d* interactions at the Fermi level are neglected, the various hyperfine contributions to the spin-lattice relaxation rate do not interfere with each other. However, in contrast to the situation in cubic metals the orbital and dipolar relaxation rates in hexagonal metals are anisotropic except when $x = 0.8$, $y = 0.5$. It should also be noted that the core-polarization reduction factor (2.32) represents a specialization of the general result $\mathrm{K}_d^{(1)} = \sum_\Gamma (f_d^\Gamma)^2 (g^\Gamma)^{-1}$, where f_d^Γ is the relative weight of *d* states at the Fermi level belonging to the representation Γ, and the normalization of the f_d^Γ is given by $\sum_\Gamma f_d^\Gamma = 1$.

We now examine the consequences of *s-d* interactions. In cubic metals such interactions have no effect on the relaxation rate since the *s* and *d* functions belong to different irreducible representations of the cubic point group (O). In the hexagonal case, on the other hand, both the $s(Y_1^0)$ and $d(Y_2^0)$ functions belong to the A_1' representation of D_{3h} and consequently to the same *m* in the expansion (2.9). Hence, matrix elements of the contact and core-polarization interactions between these functions *will* interfere provided that these functions are admixed in $\Psi_{\mu\mathbf{k}\sigma}(\mathbf{r})$ at the Fermi level. If the A_1' functions are expressed as linear combinations of the form $\xi_{\mu\mathrm{k}} Y_1^0 + (1-\xi_{\mu\mathrm{k}}^2)^{1/2} Y_2^0$, the resulting interference term is given by

$$R_{s-d} = (8\pi/\hbar)(\gamma_n\hbar)^2 k_B [N(0)]^2 H_{\mathrm{hfs}}^{(s)} H_{\mathrm{hfs}}^{(d)} \times \langle (F_{\mu\mathrm{k}}^{\Gamma(A_1')})^2 \xi_{\mu\mathrm{k}}^2 (1-\xi_{\mu\mathrm{k}}^2) \rangle, \quad (2.41)$$

where the angular brackets denote an average over the Fermi surface. Since $H_{\mathrm{hfs}}^{(s)}$ and $H_{\mathrm{hfs}}^{(d)}$ are of opposite sign $(H_{hfs}^{(d)} < 0)$ this term interferes *destructively* with (2.25).

The variation of the reduction factors $\mathrm{K}_d^{(1)}$, $\mathrm{K}_{\mathrm{orb}}^{(1)}$, and $\mathrm{K}_{\mathrm{orb}}^{(1)} + \mathrm{K}_{\mathrm{orb}}^{(2)}$ with the orbital admixture coefficients *x* and *y* is illustrated in Figs. 1, 2, and 3, respectively. (The dipolar contribution is small, as is also the case in cubic metals, and will therefore be ignored in the following.) The behavior of these factors reveals three important differences in the relaxation rate between cubic and hexagonal transition metals.

(1) The most obvious difference lies in the number of *d*-electron orbital admixture parameters which appear in the theory. In cubic metals the *d*-band properties are specified by a single admixture parameter. In hexagonal metals, two parameters are required as a result of the lower symmetry.

(2) The orbital contribution to the relaxation rate in hexagonal metals is dependent on field orientation. This anisotropy is particularly large when *y* is very small and *x* is large. The anisotropy vanishes for $x = 0.8$, $y = 0.5$ since the various *d* orbitals in that case have equal admixture coefficients in the wave function (spherical Fermi surface). The orbital and core-polarization reduction factors are then identical to the corresponding factors for cubic metals.

(3) In general, the sum of orbital and core-polarization rates is not as independent of the orbital admixture coefficients as is the case in cubic metals. The lack of sensitivity to the orbital character of the wave function in cubic systems is associated with the fact that the absolute magnitudes of $H_{\mathrm{hfs}}^{(d)}$ and $H_{\mathrm{hfs}}^{(\mathrm{orb})}$ are often nearly the same. The *d*-band contribution to the re-

---

[8] See, for example, A. K. Saha and T. P. Das, *Theory and Applications of Nuclear Induction* (Saha Institute of Nuclear Physics, Calcutta, India, 1957), p. 252.

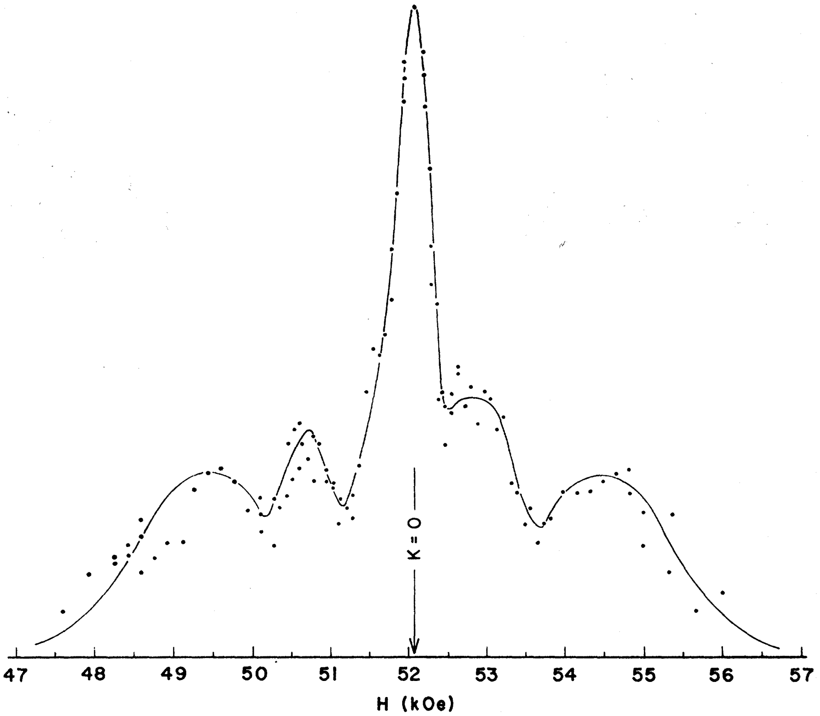

FIG. 4. Plot of observed spin-echo intensity in titanium metal due to ^{47}Ti and ^{49}Ti at 1.95°K as a function of magnetic field strength ($\nu = 12.500$ MHz). The data were obtained with a two equal-width (20 μsec) pulse sequence. The pulse separation was $\tau = 10$ msec. The arrow indicates the zero Knight shift field strength.

laxation rate is therefore nearly proportional to $K_d^{(1)} + K_{\text{orb}}^{(1)}$. The reduction factors for cubic symmetry are[1,2]

$$K_d^{(1)} = \tfrac{1}{3}x^2 + \tfrac{1}{2}(1-x)^2, \tag{2.42}$$

$$K_{\text{orb}}^{(1)} = \tfrac{2}{3}x[2-(5/3)x], \tag{2.43}$$

where x is the average fractional Γ_5 character of the d functions at the Fermi level. Hence,

$$K_d^{(1)} + K_{\text{orb}}^{(1)} = \tfrac{1}{2} + \tfrac{1}{3}x[1-(5/6)x], \tag{2.44}$$

which depends only weakly on x. An inspection of the corresponding expression (2.32)+(2.34) shows that this weak dependence does not hold for the hexagonal case.

The foregoing analysis contains two tacit assumptions. In the first place, it was assumed that the expansion of the conduction-electron wave functions at the Fermi level could be limited to $l=0$ and $l=2$ atomic functions [i.e., $N(0) = N_s(0) + N_d(0)$]. It is likely, however, that the $l=1$ admixture is often comparable to the $l=0$ admixture. Nevertheless, the $l=1$ hyperfine interaction may be safely neglected since p hyperfine fields are generally quite small compared to s and d hyperfine fields. The major effect of an appreciable p admixture at the Fermi level is therefore to reduce $N(0)$ relative to the total bare-electron density of states by an amount which is proportional to the fractional p character. This reduction is probably small since the density of states is dominated in transition metals by the d-band contributions. {Alternatively, the p admixture may be viewed as part of an effective s density provided that the contact hyperfine field is reduced by the factor $N_s(0)/[N_s(0)+N_p(0)]$.} A potentially more serious defect in the analysis is the assumption that the three d orbitals (2.16)–(2.18) have identical radial dependences. In other words, the d-spin and d-orbital hyperfine fields in (2.4) and (2.6), respectively, are assumed to be constants. This assumption is reasonable only if the potential within the atomic volume is nearly spherically symmetric.

III. EXPERIMENTAL TECHNIQUES

During the course of the present work, powdered titanium specimens from three sources[9] were studied. No discernible differences were detected in the results of nuclear-magnetic-resonance measurements on these specimens. The hcp structure of the samples was verified by powder x-ray diffraction techniques. The experimental results presented in Sec. IV were obtained on the Johnson-Matthey titanium sponge. According to the supplier, the principal impurities as determined by spectrographic analysis were (in ppm) Sn-100, Na-100, Fe-70, Si-3, and Mn-1. Other metallic impurities were not detected. Powdered samples were prepared by ball-milling the sponge in deionized water until a sufficient amount of 200-mesh material had been accumulated. The power was leached with dilute HCl in order to remove surface contaminations. It was then

---

[9] Gallard Schlesinger Chemical Manufacturing Corporation (granules-B3447, 99.9+%); Johnson, Matthey, and Company, Limited (Sponge, 99.9+%, Lot No. S.2692); Bureau of Mines (Electrolytic, powder, 99+%), we are indebted to Dr. R. A. Forman for making this sample available to us. The purity estimates given here do not include possible contamination by oxygen and nitrogen.

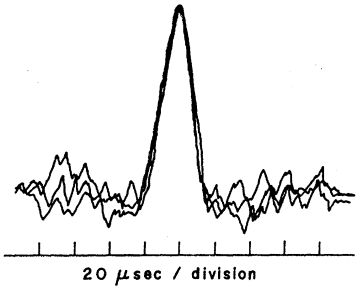

FIG. 5. Examples of typical spin echos observed at 52.2 kOe ($\nu = 12.500$ MHz) under the same experimental conditions as were used to obtain the data in Fig. 4.

placed in a vacuum furnace at 6×10^{-6} Torr and annealed for 6 h at 700°C. The vacuum was maintained in the 10^{-6} Torr range during the entire heating cycle. This was accomplished by raising the temperature gradually over several hours from room temperature to the 700°C annealing temperature. The nuclear-resonance measurements were performed on samples which had been diluted with 325-mesh NaCl powder to provide the necessary electrical insulation between the titanium particles.

The nuclear-resonance measurements were carried out by standard crossed-coil transient techniques in the temperature range 1–4°K at frequencies near 12 MHz. The magnetic field was provided by a compensated 60-kOe superconducting solenoid. Sample temperatures were controlled by regulated pumping on liquid helium contained in a separate sample Dewar.

Transient excitation of the nuclear resonance was provided by a 15-kW gated rf amplifier. Rotating fields in excess of 50 Oe were easily achieved. Because of the extreme inhomogeneous width (>8 kOe) of the nuclear resonance resulting from the electric field gradient at the titanium nuclei, all measurements were based on observations of the spin echo following two equal-width rf pulses. Phase-coherent detection was employed in order to assure detector linearity. The detector output was displayed on an oscilloscope and recorded photographically.

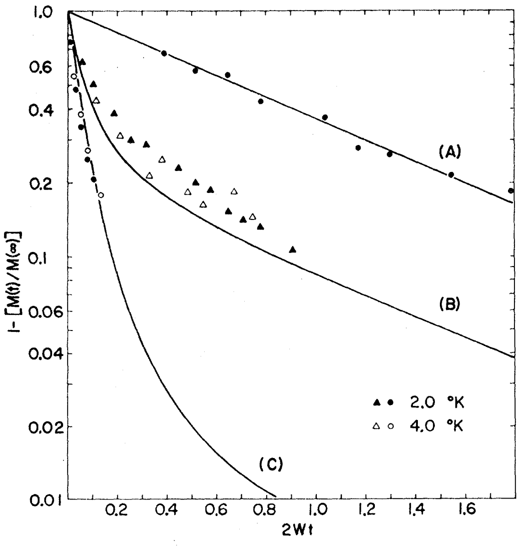

FIG. 6. Comparison of experimental and theoretical spin-lattice relaxation curves for titanium metal for $T_1T = 150$ sec°K ($2W = T_1^{-1}$). The three cases (A), (B), and (C) are discussed in the text.

TABLE I. Summary of magnetic hyperfine fields and spin-lattice-relaxation rates $\mathcal{R}_i = 2h\gamma_n^2 k_B[N(0)H_{\mathrm{hfs}}^{(i)}]^2$ in titanium metal.

	$H_{\mathrm{hfs}}^{(i)}$ (10^6 Oe)	$\mathcal{R}_i$ (sec °K)$^{-1}$
Contact	+1.0	0.807
Core polarization	−0.10	0.00807
Orbital	+0.16	0.0206

The enormous width of the nuclear resonance not only resulted in a relatively poor signal-to-noise ratio but also made it exceedingly difficult to obtain accurate spin-lattice relaxation rates. The usual technique in which the recovery of the nuclear magnetization is observed after application of a saturating "comb" of rf pulses was only partially successful. Complete saturation could not be achieved even with pulse trains of several hundred 5–10 μsec rf pulses. Since the spin-lattice relaxation times T_1 were of the order of a minute it appeared feasible to achieve saturation by a less drastic method. Two methods were considered. In

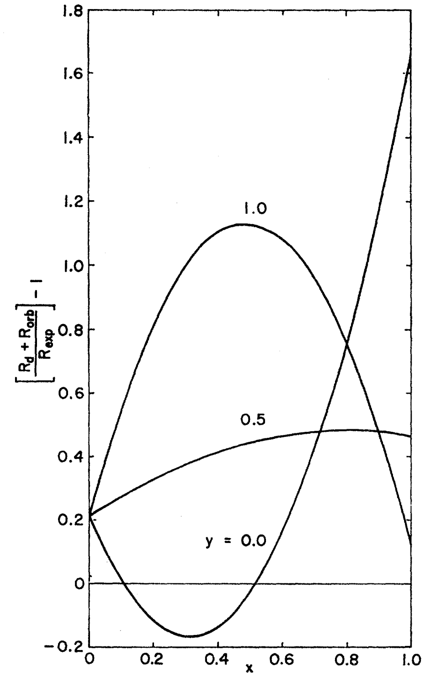

FIG. 7. Plot of the d-electron contributions ($\rho = 0$) to the spin-lattice relaxation rate in titanium metal as a function of the orbital-admixture parameters x and y.

principle, the easiest approach is to use a low-power cw sweep oscillator as the source of rf excitation. Saturation should be attainable with several frequency sweeps across the inhomogeneously broadened resonance during a time less than T_1. In the present case, however, it was more convenient to demagnetize the sample by removing it from the magnet.[10] This was accomplished by mounting the sample probe on a motor driven hoist. Isolation between the helium Dewar and the atmosphere was achieved by means of a sliding O-ring seal. A stroke of 10 in. was sufficient to reduce the field strength at the sample to about 3% of its value at the center of the magnet. Care was taken that the sample remained in the helium bath at all times. The sample was left in the "out" position for several T_1's. Upon reinsertion into the magnet, the recovery of the nuclear magnetization was monitored in the usual way. The time required for insertion was 0.7 sec.

IV. EXPERIMENTAL RESULTS

A. Nuclear-Resonance Line Shape

The abundant magnetic isotopes of titanium are ^{47}Ti ($\mu_N = -0.78711$ nm, $I = \frac{5}{2}$)[11] and ^{49}Ti($\mu_N = -1.1022$ nm, $I = \frac{7}{2}$)[11] which occur in natural abundances of 7.75 and 5.51%, respectively. The gyromagnetic ratios are nearly identical, the frequency-field ratios being 0.2400 kHz/Oe for ^{47}Ti and 0.2401 kHz/Oe for ^{49}Ti. This small difference was undetectable in the present experiments and the observed signals were therefore superpositions of the ^{47}Ti and ^{49}Ti resonances. The electric quadrupole moments of the two isotopes are not known but have been estimated to lie in the range $(0.3\text{–}0.4) \times 10^{-24}$ cm^2.[12]

The hcp structure generally produces nonvanishing electric field gradients at the nuclear sites. The resulting first-order quadrupole broadening of the nuclear-resonance spectrum ($I > \frac{1}{2}$) in powder specimens is particularly large in titanium metal. This undoubtedly accounts for the fact that the nuclear resonance has not been observed previously in this metal. Figure 4 shows an experimental spectrum obtained at a frequency of 12.500 MHz and a temperature of 1.95°K using rf pulse widths of 20 μsec. (Experiments with 100-μsec pulse widths yielded identical results within the experimental uncertainty.) The data points represent measured echo intensities as a function of magnetic field strength. Each point is an average of three independent photographic observations. (Typical echos are shown in Fig. 5.) A time interval of 2 min separated successive "shots." The most prominent feature of the spectrum (Fig. 4) is the strongly peaked central portion which presumably corresponds to the $+\frac{1}{2} \leftrightarrow -\frac{1}{2}$ transitions of ^{47}Ti and ^{49}Ti. The total number of satellite pairs expected for ^{47}Ti ($I = \frac{5}{2}$) is two, while the corresponding number for ^{49}Ti ($I = \frac{7}{2}$) is three. The first-order shifts of the satellites for a symmetric field gradient q are conveniently expressed for any spin I in terms of the quadrupole frequency[13]

$$\nu_Q = h^{-1} e^2 qQ \left[\frac{3}{2I(2I-1)} \right], \tag{4.1}$$

where Q is the nuclear electric quadrupole moment. The frequency shift of the peaks in the powder pattern associated with $m \leftrightarrow m-1$ transitions is given by

$$\nu_m^{(1)} = \tfrac{1}{2}(m - \tfrac{1}{2}) \nu_Q. \tag{4.2}$$

The closest-spaced pair of satellites is reasonably well resolved in the observed spectrum. The splitting is approximately 2.3 kOe. The remaining pairs are contained in the broad wings of the spectrum. The shift of the central transition toward higher fields relative to the mean position of the satellites is due to second-order quadrupole effects.

The observed quadrupole structure cannot be interpreted with complete certainty since the ratio of the electric quadrupole moments Q^{47}/Q^{49} is not known. The partial resolution of the satellite spectrum suggests, however, that the respective quadrupole frequencies ν_Q are either nearly identical or integral multiples of one another. This follows from (4.1) since the factor in brackets has the value 3/20 for $I = \frac{5}{2}$ and 3/42 for $I = \frac{7}{2}$. Thus, if the quadrupole moments of ^{47}Ti and ^{49}Ti are approximately equal we can assign the closest-spaced satellite pair to the ^{49}Ti ($\pm\frac{1}{2} \leftrightarrow \pm\frac{3}{2}$) transitions. The wings of the observed spectrum contain the remaining satellites in three distinct sets which are not resolved, however, in the present experiment. The first set consists of the ^{47}Ti ($\pm\frac{1}{2} \leftrightarrow \pm\frac{3}{2}$) and ^{49}Ti ($\pm\frac{3}{2} \leftrightarrow \pm\frac{5}{2}$) transitions. The next set arises from the ^{49}Ti ($\pm\frac{5}{2} \leftrightarrow \pm\frac{7}{2}$) transitions while the ^{47}Ti ($\pm\frac{3}{2} \leftrightarrow \pm\frac{5}{2}$) transitions give rise to the satellite pair having the largest splitting (9.2 kOe). The calculated spacings and intensities of the satellites based on the above assignments are in satisfactory agreement with the observed spectrum if $h^{-1}e^2qQ^{47} \approx h^{-1}e^2qQ^{49} \approx 7.7$ MHz. This assignment is supported by the magnitude of the observed second-order broadening and shift of the $+\frac{1}{2} \leftrightarrow -\frac{1}{2}$ transitions. The calculated second-order splittings are 0.60 kOe (^{47}Ti) and 0.28 kOe (^{49}Ti), while the calculated shifts of the high-field component are 0.38 kOe (^{47}Ti) and 0.17 kOe (^{49}Ti). These values are quite consistent with the observed asymmetry of the central component. Another possible assignment is obtained by assuming that the $\pm\frac{1}{2} \leftrightarrow \pm\frac{3}{2}$ transition of the two isotopes nearly coincide. This requires $h^{-1}e^2qQ^{47} \approx 3.7$ MHz and $h^{-1}e^2qQ^{49} \approx 7.7$ MHz and thus a factor-of-2 difference in the quadrupole moments which appears somewhat unlikely. This

---

[10] This technique was suggested to the author by Professor M. Weger and Professor W. G. Clark.

[11] C. D. Jeffries, Phys. Rev. **92**, 1262 (1953).

[12] M. J. Weber and R. R. Allen, J. Chem. Phys. **38**, 726 (1963).

[13] See M. H. Cohen and F. Reif [in *Solid State Physics*, edited by F. Seitz and D. Turnbull (Academic Press Inc., New York, 1957, Vol. 5,] for an excellent review of nuclear quadrupole effects in solids.

assignment also fails to account for the large second-order shift of the central transition.

The Knight shift in titanium metal can be estimated from the center of gravity of the satellite spectrum. We obtain $K=(+0.4\pm0.2)\%$. This value is consistent with the observed position of the central transition. In view of the noncubic symmetry of titanium the Knight shift contains both isotropic (K_{iso}) as well as anisotropic (K_{ax}) terms.[14] (In general, $|K_{\text{iso}}|>|K_{\text{ax}}|$.) Unfortunately, these contributions could not be distinguished in our experiments because of the complexity of the resonance spectrum.

B. Spin-Spin Relaxation

The observed transverse relaxation times T_2 in titanium metal are much longer than the calculated rigid-lattice dipolar relaxation time of approximately 6 msec. Of course, the calculated value of T_2 is only valid in the absence of inhomogeneous broadening. In titanium, however, the different $\Delta m=\pm1$ transitions are completely detuned (except in crystal grains for which $\theta=\cos^{-1}3^{-1/2}$) and energy conservation requirements therefore limit simultaneous nuclear spin-flip transitions to pairs of adjacent levels. The probability of such transitions occurring is thus greatly reduced, and T_2 becomes quite long. The experimental transverse relaxation times were obtained for the central part of the quadrupole spectrum from measurements of echo phase-memory decays. The echo amplitudes were found to decrease nearly exponentially with increasing pulse separation τ in a two-pulse sequence. The $1/e$ times of the echo intensity-versus-2τ plots were somewhat dependent on rf pulse amplitude and varied between 100 and 200 msec. No temperature dependence was detected.

C. Spin-Lattice Relaxation

As mentioned earlier, the severe quadrupole broadening of the titanium resonance interfered seriously with the measurement of the spin-lattice relaxation time T_1. Figure 6 summarizes some of the experimental data. The recovery of the nuclear magnetization only followed an exponential time dependence when the hoist technique was applied [case (A)], since it was impossible in the present experiments to achieve an initial state of unique spin temperature by rf saturation techniques. In the temperature range 1–4°K, the relaxation time was found to be inversely proportional to the absolute temperature with

$$T_1T=150 \text{ sec °K}.$$

The estimated uncertainty is $\pm15\%$. Although most of our relaxation experiments were restricted by signal-to-noise considerations to the central transition, a few measurements were also made on the satellite transitions. Within our experimental error the measured satellite relaxation times, as determined by the hoist technique, were the same as for the central transition.

It is of interest to examine the behavior of the relaxation curves following rf saturation of the central transition. The solid curves in Fig. 6 are theoretical predictions for different initial states of the nuclear spin system. The details of the calculations are given in the Appendix. Curve (C) assumes a very short comb of sufficient spectral purity to saturate completely the $+\frac{1}{2}\leftrightarrow-\frac{1}{2}$ transitions of both isotopes but have no effect on the populations of the other spin levels. Curve (B) assumes a comb of sufficient duration to allow the populations of the $|m|>\frac{1}{2}$ levels to attain thermal equilibrium with those of the $|m|=\frac{1}{2}$ levels. In other words, immediately after the comb, the $+\frac{1}{2}\leftrightarrow-\frac{1}{2}$ transition is saturated (infinite-spin temperature) while the population differences between all other pairs of adjacent levels are determined by the lattice temperature. This assumes, of course, that spectral spin diffusion due to cross relaxation between different intervals can be ignored. The data associated with the calculated curves were obtained as follows: (B) comb duration $\sim T_1$, comb composed of 100 8-μsec pulses; (C) comb duration 0.1 sec, comb composed of 40 10-μsec pulses. The agreement between theory and experiment is extremely good for (C). The agreement is somewhat poorer in the case of (B), presumably because the comb did not quite yield the assumed initial state of the spin system. It is likely, for example, that the comb raised the spin temperature of the $(\pm\frac{1}{2},\pm\frac{3}{2})$ level pairs to some extent. This follows from the fact that the length of the comb would have been insufficient to thermalize the satellite transitions if only spin-lattice relaxation processes had been available to redistribute the spin populations. The neglect of spectral diffusion during the recovery period, on the other hand, is justified since even the initial relaxation rate was observed to be directly proportional to the lattice temperature. The effectiveness of spin-spin relaxation processes is therefore limited to the establishment of a Boltzmann distribution for the relative populations of adjacent spin levels. The recovery of the multilevel spin system as a whole toward internal equilibrium characterized by a single spin temperature is dependent on spin-lattice relaxation processes.

The qualitative difference between cases (B) and (C) is of considerable practical importance when the hoist technique (or equivalent technique) is impractical. In many experimental determinations of T_1 accurate measurements of the recovery curves are limited to approximately the first decade because of limited signal-to-noise ratios. In this range the nonexponential behavior of (C) is not very evident. It is then easy to mistake the observed recovery for the true spin-lattice recovery $M(t)/M(\infty)\propto1-\exp(-t/T_1)$. Such an error resulted in a preliminary value[15] of T_1T

---

[14] See, for example, W. H. Jones, Jr., T. P. Graham, and R. G. Barnes, Phys. Rev. **132,** 1898 (1963).

[15] A. Narath, Bull. Am. Phys. Soc. **11,** 220 (1966).

for titanium metal which is much smaller than that obtained in the present work. The same difficulties have been encountered for the hexagonal Group-III transition metals scandium (^{45}Sc: $I=\frac{7}{2}$; $h^{-1}e^2qQ=2.0$ MHz[16]) and lanthanum (^{139}La: $I=\frac{7}{2}$, $h^{-1}e^2qQ=7.8$ MHz[17]). Measurements of T_1 for yttrium[18] (Y: $I=\frac{1}{2}$, $h^{-1}e^2qQ=0$) gave surprisingly long relaxation times when compared to the reported values[19] for the other two metals in this group. Making use of experience gained in our study of titanium we have remeasured T_1 in these metals and have obtained relaxation times which are about an order of magnitude longer [$T_1T(^{45}\mathrm{Sc})=1.6$ sec °K,[20] $T_1T(^{139}\mathrm{La})=0.58$ sec °K[20]] than the previous values. Under conditions of extreme inhomogeneous broadening it is therefore of great advantage to make use of case (B). The initial recovery is then quite nonexponential and the asymptotic limit is reached much more quickly than in (C). If the second-order quadrupole broadening is small it may be more convenient to achieve case (B) by means of cw saturation of the central transition for a time equal to several T_1's than to rely on extremely long-rf combs.

V. DISCUSSION

A. Quadrupole Interaction

The quadrupole coupling constant $h^{-1}e^2qQ^{47,49}\approx 7.7$ MHz in titanium metal is surprisingly large. For example, in scandium metal $h^{-1}e^2qQ^{45}=2.0$ MHz,[16] with $Q^{45}\approx 0.2\times 10^{-24}$ cm^2.[21] If $Q^{47,49}\approx 0.4\times 10^{-24}$ cm^2, the electric field gradient q would still have to be twice as large in titanium as in scandium. Three important contributions to q are commonly recognized in metals.[22] The first is the direct lattice field gradient (q_{latt}) which arises from the incompletely screened positive-ion cores. A second contribution (q_{loc}) is believed to arise from the nonspherical distribution of conduction electrons within the atomic volume surrounding the nuclear site. Finally, one needs to consider the contribution arising from the closed shells which become distorted under the influence of the nonspherical potential associated with q_{latt} and q_{loc}. This contribution is usually expressed in terms of the Sternheimer antishielding factors[23] γ_∞ and R_0, respectively. The total field gradient may therefore be written

$$q=q_{\mathrm{latt}}(1-\gamma_\infty)+q_{\mathrm{loc}}(1-R_Q), \tag{5.1}$$

where $(1-\gamma_\infty)$ is approximately $+8$ for both scandium and titanium and $1-R_Q$ is probably near unity. The magnitude of q_{latt} may be estimated by interpolation of de Wette's[24] numerical results for the hcp lattice. Using $c/a=1.601$ and $a=2.953$ Å for titanium, we find $Z^{-1}q_{\mathrm{latt}}=+5.7\times 10^{21}$ cm^{-3}, where Z is the effective charge of the ion cores. This value is essentially identical to the value $Z^{-1}q_{\mathrm{latt}}=+5.0\times 10^{21}$ cm^{-3} reported by Barnes *et al.*[16] for scandium ($c/a=1.5936$, $a=3.309$ Å). If one makes the naive assumption that Z is equal to the number of valence electrons [$Z(\mathrm{Ti})=+4$, $Z(\mathrm{Sc})=+3$], one obtains a value of 1.5 for the ratio $q_{\mathrm{latt}}(\mathrm{Ti})/q_{\mathrm{latt}}(\mathrm{Sc})$. This is fortuitously close to the required ratio. Actually the ion-core charge is probably much smaller than assumed above because of the strong localization of the d electrons. Furthermore, even for the extreme choice of $Z=+3$, the calculated quadrupole coupling constant in scandium has a value which is only 44% of the experimental value.[16] It appears, therefore, that the observed coupling constants must be dominated by q_{loc}. Since this quantity cannot at present be calculated it is not possible to draw further conclusions from our data.

B. Spin-Lattice Relaxation

We now return to the main topic of this paper, namely, the nuclear spin-lattice relaxation behavior of hcp transition metals. In this section, we apply the theory developed in Sec. II to the experimental relaxation rate of titanium metal. Because of the large number of parameters which are contained in the theoretical rate equation (2.25), it is, of course, not possible to obtain a unique fit to the experimental relaxation rate. Our aim instead is to estimate the acceptable ranges for the least known parameters and in this way examine the sensitivity of the calculated rates to changes in the various parameters.

The relevant hyperfine fields for titanium metal are listed in Table I. They were estimated in the following way. The orbital hyperfine field per unit orbital angular momentum is given to a good approximation by $H_{\mathrm{hfs}}^{(\mathrm{orb})}=-\gamma_e\hbar\langle r^{-3}\rangle$, as noted earlier, and $\langle r^{-3}\rangle$ represents an average over the radial distribution of the d electrons near the Fermi surface. We assume that $\langle r^{-3}\rangle$ may be approximated by its value in the neutral titanium atom.[25] The core-polarization hyperfine field per electron can be estimated because of the near constancy[25] of $H_{\mathrm{hfs}}^{(d)}$ among $3d$ transition-metal ions.[26]

---

[16] R. G. Barnes, F. Borsa, S. L. Segel, and D. R. Torgeson, Phys. Rev. **137**, A1828 (1965).

[17] A. Narath (to be published).

[18] A. T. Fromhold, Jr., and A. Narath, Bull. Am. Phys. Soc. **10**, 606 (1965).

[19] Y. Masuda, J. Phys. Soc. Japan **19**, 239 (1964).

[20] A. Narath and A. T. Fromhold, Jr., Phys. Letters **25**, 49 (1967).

[21] G. Fricke, H. Kopfermann, S. Penselin, and K. Schlüpmann, Naturwiss. **46**, 106 (1959).

[22] R. E. Watson, A. C. Gossard, and Y. Yafet, Phys. Rev. **140**, A375 (1965).

[23] R. Sternheimer, Phys. Rev. **84**, 244 (1951).

[24] F. W. de Wette, Phys. Rev. **123**, 103 (1961).

[25] A. J. Freeman and R. E. Watson, in *Magnetism*, edited by G. T. Rado and H. Suhl (Academic Press Inc., New York, 1965), Vol. IIA, Chap. IV.

[26] A major uncertainty arises, however, because of the unknown contribution to $H_{\mathrm{hfs}}^{(d)}$ from the d-spin exchange polarization of the 4s component of the conduction electrons. This contribution is presumably positive (Ref. 25) and would thus have the effect of reducing the absolute magnitude of $H_{\mathrm{hfs}}^{(d)}$. [See for example the discussion by W. E. Gardner and J. Penfold, Phil. Mag. **11**, 549 (1965).] Because of the uncertainties involved we ignore this effect here.

Finally, we obtain an approximate value for the contact hyperfine field by adjusting an earlier estimate for vanadium metal[1] according to known trends in the magnitude of $H_{\mathrm{hfs}}^{(s)}$ among $3d$ atoms.

The density of states at the Fermi level, for one direction of the spin, may be calculated in the independent-particle approximation from

$$N(0)=\tfrac{3}{2}(\pi k_B)^{-2}\gamma_{\mathrm{el}}, \tag{5.2}$$

where γ_{el} is the electronic specific-heat coefficient. Using the specific-heat data of Kneip *et al.*[27] and Dummer,[28] we find $N(0)=4.43\times10^{11}$ erg^{-1} atom^{-1}.

Thus the problem of calculating the relaxation rate has been reduced to a determination of (1) the s/d ratio, (2) the orbital admixture coefficients x and y, (3) the electron-phonon enhancement of the electronic specific heat, and (4) the magnitude of the s-d interference term (2.41). In the absence of interference effects, the total relaxation rate is given by the sum of the individual magnetic hyperfine contributions. These contributions are proportional to

$$\mathcal{R}_i=2h\gamma_n^2k_B[N(0)H_{\mathrm{hfs}}^{(i)}]^2, \tag{5.3}$$

so that the total rate may be written as

$$R=\mathcal{R}_s\rho^2+[\mathcal{R}_d\mathrm{K}_d^{(1)}+\mathcal{R}_{\mathrm{orb}}(\mathrm{K}_{\mathrm{orb}}^{(1)}+\mathrm{K}_{\mathrm{orb}}^{(2)}\sin^2\theta)]\times(1-\rho)^2. \tag{5.4}$$

The dipolar term has been ignored in (5.4) because of its small magnitude. Values of $\mathcal{R}_i$ computed on the basis of the above hyperfine-field estimates are listed in Table I. A comparison of the calculated values of $\mathcal{R}_i$ with the experimental rate $R_{\mathrm{exp}}=0.0067$ (sec °K)$^{-1}$ reveals immediately the strong transition-metal character of titanium since the calculated rate would exceed the experimental rate by two orders of magnitude if $\rho=1$. Even in the limit $\rho=0$, the rate would be grossly overestimated were it not for the reduction factors in (5.4). The effect of these factors is illustrated in Fig. 7 which shows the dependence of the d-electron rate [the bracketed term in (5.4)] on the orbital admixture coefficients. Since the experimental measurements were carried out on a powder, the $\sin^2\theta\mathrm{K}_{\mathrm{orb}}^{(2)}$ term in (5.4) was replaced by its average value $\frac{2}{3}\mathrm{K}_{\mathrm{orb}}^{(2)}$. This simplification is justified by the fact that anisotropy in the orbital relaxation rate would probably have escaped detection in the present experiments.

Figure 7 reveals two striking features. In the first place, the calculated rates are seen to be strong functions of the orbital admixture parameters. Secondly, the calculated d-electron rates exceed the experimental rate for most values of x and y. Thus, even in the unlikely event that $\rho\approx0$, agreement with experiment can only be achieved over an extremely limited range of x and y values. In fact, it appears that $\rho\approx0.1$ is a more appropriate choice for titanium. For example, combining an estimate for the orbital magnetic susceptibility of titanium ($\chi_{VV}=73\times10^{-6}$ emu/mole) given by Shimizu *et al.*[29] with the orbital hyperfine field in Table I according to

$$K_i=(\mu_BN)^{-1}H_{\mathrm{hfs}}^{(i)}\chi_i, \tag{5.5}$$

where N is Avogadro's number and μ_B is the Bohr magneton, we obtain $K_{VV}=+0.20\%$. This value is in essential agreement with our measured value of the total Knight shift $K=+0.4\pm0.2\%$. Since $K_s=+1.4\%$ for $\rho=1(\chi_{\mathrm{spin}}=81\times10^{-6}$ emu/mole[29]), it is apparent that the contact shift must be nearly cancelled by the core-polarization shift. Since $|H_{\mathrm{hfs}}^{(d)}/H_{\mathrm{hfs}}^{(s)}|\approx0.1$ we are immediately led to the conclusion that $\rho\approx0.1$ as stated above. For this value of ρ we calculate $R_s=0.008$ (sec °K)$^{-1}$ which is somewhat faster than the experimental rate.

The apparent discrepancy between theory and experiment is probably a consequence of one or both of the following effects:

(1) The density of states $N(0)$ may have been overestimated. A 40–70% electron-phonon enhancement of the electronic specific heat would be sufficient to remove the disagreement.

(2) The d functions at the Fermi level may be predominantly of the A_1' symmetry type (i.e., small x). Hence, if the s and d bands are strongly admixed at the Fermi level the s-contact and $d(A_1')$ core-polarization contributions to the relaxation rate would largely cancel one another. It is also possible, of course, that one or more of the hyperfine fields were overestimated by a significant amount. This explanation appears less plausible, however, in view of the relatively large positive Knight shift.

It is not possible, on the basis of available information, to distinguish between the two alternative explanations given above. In all probability, both effects are important. In this connection it is significant that Clogston[30] has obtained an estimate of 70% for the electron-phonon enhancement of the electronic specific heat of scandium. It would be somewhat surprising, however, if the enhancement factor for titanium (whose electronic specific heat is only one-third that of scandium) had the same magnitude.

In conclusion, it has been shown that the detailed nuclear-spin-lattice-relaxation behavior of hexagonal transition metals is much more strongly influenced by the symmetry properties of the d functions at the Fermi surface than is the case in cubic transition metals. Two additional differences arise because of the lower symmetry of the hexagonal lattice. These are (1) the anisotropy of the orbital and dipolar relaxation rates

---

[27] G. D. Kneip, Jr., J. O. Betterton, Jr., and J. O. Scarbrough, Phys. Rev. **130**, 1687 (1963).

[28] G. Dummer, Z. Physik **186**, 249 (1965).

[29] M. Shimizu, T. Takahashi, and A. Katsuki, J. Phys. Soc. Japan **18**, 1192 (1963).

[30] A. M. Clogston, Phys. Rev. **136**, A8 (1964).

and (2) the occurrence of destructive interference between the contact rate and the $d(A_1')$ component of the core-polarization rate if the corresponding functions are admixed at the Fermi level. Although this increased complexity interferes with the detailed interpretation of the experimental rates it should provide a stimulus for interesting future investigations. For example, it appears feasible to obtain estimates of ρ, and the orbital admixture coefficients from known band structures by means of tight-binding interpolation schemes.[31] Reliable band structures for this purpose obtained by either augmented-plane-wave (APW) or Korringa-Kohn-Rostoker (KKR) methods are becoming available. Finally, it would be of interest to measure T_1's in single crystals of hcp transition metals in order to detect the anisotropy of the orbital relaxation mechanism.

ACKNOWLEDGMENTS

It is a pleasure to acknowledge the expert technical assistance of D. C. Barham. The author is also grateful to J. E. Hesse for his help in sample preparation.

APPENDIX

We wish to derive expressions which describe the relaxation behavior of the $+\frac{1}{2}\leftrightarrow-\frac{1}{2}$ transition for nuclear-spin systems having $I=\frac{5}{2}$ and $I=\frac{7}{2}$ under the assumption that the energy levels are unequally spaced so that simultaneous nuclear spin-flips involving two different transitions are forbidden by energy conservation requirements. Furthermore, we assume that the transition probability per unit time $W_{m,m'}$ due to nuclear spin-lattice interactions is of the form

$$W_{m,m'}=W[|\langle m'|I^+|m\rangle|^2+|\langle m'|I^-|m\rangle|^2]. \qquad \text{(A1)}$$

The selection rule on m' is therefore $m'=m\pm1$. We let $N_m(t)$ be the population of the mth state at a time t and $N_m{}^0$ the corresponding thermal equilibrium population. The relative deviation from equilibrium may then be denoted by $n_m(t)=[N_m(t)-N_m{}^0]/\sum_m N_m{}^0$. Defining a quantity which is proportional to the magnetization of adjacent pairs of spin levels

$$a_m(t)=[n_m(t)-n_{m-1}(t)], \qquad \text{(A2)}$$

the relaxation behavior of the spin system is specified by the $2I$ coupled-linear-differential equations[32–34]

$$da_m(t)/dt=W\sum_{m'}A_{m,m'}a_{m'}(t). \qquad \text{(A3)}$$

The nonvanishing elements of **A** are given by

$$A_{m,m+1}=[I(I+1)-m(m+1)], \qquad \text{(A4)}$$

$$A_{m,m}=-2[I(I+1)-m(m-1)], \qquad \text{(A5)}$$

$$A_{m,m-1}=[I(I+1)-(m-1)(m-2)]. \qquad \text{(A6)}$$

The solution of (A3) has the form

$$a_m(t)=\sum_{m'}\alpha_{mm'}\exp(-\lambda_{m'}t), \qquad \text{(A7)}$$

where the λ_m/W are the eigenvalues of **A** and the $\alpha_{mm'}$ are components of the corresponding eigenvectors. Andrew and Turnstall[33] have obtained the general solution

$$\lambda_m/W=(m+I)(m+I+1), \qquad \text{(A8)}$$

where $m=-I+1,\cdots,+I$. The normalization of the eigenvectors is determined by the initial state of the spin system. Thus, if we define a vector $\mathbf{n}$ according to

$$\alpha_{mm'}\equiv C_{mm'}\eta_{m'}, \qquad \text{(A9)}$$

we find, using (A7)

$$\eta_{m'}=\sum_{m''}(C^{-1})_{m'm''}a_{m''}(0), \qquad \text{(A10)}$$

where $\mathbf{C}^{-1}$ is the inverse of **C**. Hence

$$\alpha_{mm'}=C_{mm'}\sum_{m''}(C^{-1})_{m'm''}a_{m''}(0). \qquad \text{(A11)}$$

The **C** columns are therefore determined within a multiplicative constant. For the special cases of $I=\frac{5}{2}$ and $I=\frac{7}{2}$ we find[35]

$$\mathbf{C}(I=\tfrac{5}{2})=\begin{bmatrix} 1.00000 & 1.00000 & 1.00000 & 1.00000 & 1.00000 \\ 1.00000 & 0.50000 & -0.25000 & -1.25000 & -2.50000 \\ 1.00000 & 0 & -0.66666 & 0 & 3.33333 \\ 1.00000 & -0.50000 & -0.25000 & 1.25000 & -2.50000 \\ 1.00000 & -1.00000 & 1.00000 & -1.00000 & 1.00000 \end{bmatrix}, \qquad \text{(A12)}$$

---

[31] F. M. Mueller, Phys. Rev. **153**, 659 (1967).

[32] A. Sher and H. Primakoff, Phys. Rev. **119**, 178 (1960).

[33] E. R. Andrew and D. P. Turnstall, Proc. Phys. Soc. (London) **78**, 1 (1961).

[34] W. W. Simmons, W. J. O'Sullivan, and W. A. Robinson, Phys. Rev. **127**, 1168 (1962).

[35] The **C** matrix for $I=\frac{5}{2}$ has already been given by Simmons *et al.* (Ref. 34). We reproduce it here for the convenience of the reader.

$$\mathbf{C}^{-1}(I=\tfrac{5}{2})=\begin{bmatrix} 0.14285 & 0.22857 & 0.25714 & 0.22857 & 0.14285 \\ 0.35714 & 0.28571 & 0 & -0.28571 & -0.35714 \\ 0.33333 & -0.13333 & -0.40000 & -0.13333 & 0.33333 \\ 0.14285 & -0.28571 & 0 & 0.28571 & -0.14285 \\ 0.02380 & -0.09523 & 0.14285 & -0.09523 & 0.02380 \end{bmatrix}, \qquad \text{(A13)}$$

$$\mathbf{C}(I=\tfrac{7}{2})=\begin{bmatrix} 1.00000 & 1.00000 & 1.00000 & 1.00000 & 1.00000 & 1.00000 & 1.00000 \\ 1.00000 & 0.66666 & 0.16666 & -0.50000 & -1.33333 & -2.33333 & -3.50000 \\ 1.00000 & 0.33333 & -0.33333 & -0.60000 & 0.06666 & 2.33333 & 7.00000 \\ 1.00000 & 0 & -0.50000 & 0 & 1.00000 & 0 & -8.75000 \\ 1.00000 & -0.33333 & -0.33333 & 0.60000 & 0.06666 & -2.33333 & 7.00000 \\ 1.00000 & -0.66666 & 0.16666 & 0.50000 & -1.33333 & 2.33333 & -3.50000 \\ 1.00000 & -1.00000 & 1.00000 & -1.00000 & 1.00000 & -1.00000 & 1.00000 \end{bmatrix}, \qquad \text{(A14)}$$

$$\mathbf{C}^{-1}(I=\tfrac{7}{2})=\begin{bmatrix} 0.08333 & 0.14285 & 0.17857 & 0.19047 & 0.17857 & 0.14285 & 0.08333 \\ 0.25000 & 0.28571 & 0.17857 & 0 & -0.17857 & -0.28571 & -0.25000 \\ 0.31818 & 0.09091 & -0.22727 & -0.36363 & -0.22727 & 0.09091 & 0.31818 \\ 0.22727 & -0.19480 & -0.29220 & 0 & 0.29220 & 0.19480 & -0.22727 \\ 0.09615 & -0.21978 & 0.01373 & 0.21978 & 0.01373 & -0.21978 & 0.09615 \\ 0.02272 & -0.09091 & 0.11363 & 0 & -0.11363 & 0.09091 & -0.02272 \\ 0.00233 & -0.01398 & 0.03496 & -0.04661 & 0.03496 & -0.01398 & 0.00233 \end{bmatrix}. \qquad \text{(A15)}$$

The recovery of the $+\frac{1}{2}\leftrightarrow-\frac{1}{2}$ magnetization is therefore given by

$$I=\tfrac{5}{2}: a_{1/2}(t)=\alpha_{1/2,-3/2}\exp(-2Wt)$$
$$+\alpha_{1/2,1/2}\exp(-12Wt)+\alpha_{1/2,5/2}\exp(-30Wt), \qquad \text{(A16)}$$

$$I=\tfrac{7}{2}: a_{1/2}(t)=\alpha_{1/2,-5/2}\exp(-2Wt)$$
$$+\alpha_{1/2,-1/2}\exp(-12Wt)$$
$$+\alpha_{1/2,3/2}\exp(-30Wt)+\alpha_{1/2,7/2}\exp(-56Wt), \qquad \text{(A17)}$$

where the $\alpha_{m,m'}$ coefficients are obtained from (A11). The theoretical curves in Fig. 6 were obtained by combining (A16) and (A17) in the ratio of the natural abundances of ^{47}Ti and ^{49}Ti, respectively. The initial conditions on which the three curves were based are as follows

(A) $a_m(0)=\epsilon-\frac{1}{2}(m-\frac{1}{2})(h\nu_Q/k_BT)$,

(B) $a_{1/2}(0)=\epsilon$, all others zero,

(C) $a_{1/2}(0)=\epsilon$, $a_{-1/2}(0)=a_{3/2}(0)=-\frac{1}{2}\epsilon$, all others zero,

where $\epsilon=|\gamma_n\hbar H/k_BT|$. We note that only (A) yields the normal single exponential behavior with $T_1^{-1}=2W$, independent of the magnitude of ν_Q.